Mapping Paddy Cropland in Guntur District using Machine Learning and Google Earth Engine utilizing Images from Sentinel-1 and Sentinel-2

Pureti Siva Nagendram
Department of ECE, KLEF, India
sivapureti9316@gmail.com (corresponding author)

Penke Satyanarayana
Department of IOT, KLEF, India
satece@kluniversity.in

Panduranga Ravi Teja
Department of IOT, KLEF, India
praviteja@kluniversity.in

Received: 30 September 2023 | Revised: 19 October 2023 | Accepted: 28 October March 2023

 DOI: https://doi.org/10.48084/etasr.6460

ABSTRACT

Ensuring global food security necessitates vigilant monitoring of crop quantity and quality. Therefore, the reliable classification of croplands and diverse Land Covers (LC) becomes pivotal in fostering sustainable agricultural progress and safeguarding national food security. The Seasonal Crop Inventory (SCI) emerges as a strong asset. In this study, Sentinel-1 (S1) and Sentinel-2 (S2) image data were used to show varied land uses and paddy crops in Guntur district, Andhra Pradesh, India, during the 2021 growing season. Employing a technologically advanced space-based remote sensing approach, this study exploited the Google Earth Engine (GEE) and a range of classification techniques, including Random Forest (RF) and Classification Regression Trees (CART), to generate pixel-based SCI tailored to the area under investigation. The results underscored the reliability of GEE-based cropland mapping in the region, demonstrating a satisfactory level of classification accuracy, surpassing 97% across distinct time intervals in overall accuracy values, Kappa coefficients, and F1-Score.

Keywords-paddy; cropland mapping; machine learning; GEE; Sentinel-1 and Sentinel-2; Guntur

I. INTRODUCTION

Rice is ingested by more than 50% of the Earth's inhabitants, and rice paddies cover more than 10% of the total cropland worldwide. On a global scale, rice is the main contributor among plant-based sources to the discharge of greenhouse gases [1]. Precise and current data on rice production are of paramount importance in achieving food and environmental objectives and safeguarding access to water. Such a significance was particularly pronounced in Malaysia, where the main staple food is rice. To guarantee domestic nutrition supply, the Malaysian administration has established an ambition to achieve a rice Self-Sufficiency Level (SSL) of 70% [2]. To evaluate the success in attaining the SSL rice target, precise and current data is needed on cultivable rice fields and their harvestable yield. Presently, data on rice fields are obtained through field surveys, which are not comprehensive, require a significant amount of time, and lack specific spatial information.

Remote sensing technology has found an extensive application in the global mapping of rice fields. Over the past two decades, Moderate Resolution Imaging Spectroradiometer (MODIS) data, known for their frequent temporal captures, have been extensively employed for this purpose [3-4]. Although this technique can detect paddy fields, the limited spatial resolution of MODIS data (500 m) is inadequate for accurately discerning paddy fields owned by small-scale farmers in Southeast Asia, which typically span less than one hectare in size [5-8]. In recent times, there has been a notable development with the emergence of Sentinel-1 (S1) and Sentinel-2 (S2) satellites, which provide data with both high spatial resolution (10 m) and frequent temporal captures (every 12 days). In particular, the two-satellite constellation of

Sentinel-2 enhances its temporal resolution to an impressive interval of 5 days. Numerous research efforts have presented the effective utilization of S1 data for the mapping of rice fields in different nations, such as Vietnam [9-10], China [11-14], the USA and Spain [15], India [16-17], the Mediterranean region [18], Iran [19], Bangladesh [20], South Korea [21], Indonesia and Malaysia [22], Philippines [23], Thailand [1, 24], and Myanmar [25]. Simultaneously, S2 has also proven its efficiency in accurately mapping rice fields in the context of Egypt [26] and China [27-29]. Several research investigations have used the combined dataset of satellite data to effectively chart the location of rice cultivation, particularly in areas with moderate climates, such as Japan [30].

Remote sensing computational platforms, such as Google Earth Engine (GEE), offer convenient availability of datasets and algorithms, providing valuable assets for research. In addition to functions such as image compilation, cloud identification, and categorization, these tools have versatile applications in diverse processing activities. These capabilities extend to multiple domains, including agriculture, where they enable the creation of comprehensive cropland assessments on a regional or national scale, as well as in areas related to climate change analysis. In previous studies, traditional techniques were often used to cover limited geographic extents. It should be noted that the synergistic potential of microwave satellite data alongside optical data for paddy field mapping has not been fully exploited in the context of satellite imagery across a substantial region. Within the framework of the Agricultural Transformation Agenda (ATA), a governmental initiative in Andhra Pradesh, there is a persistent priority to devise and execute innovative strategies to map paddy fields under the Seasonal Crop Inventory (SCI). The convergence of recent advancements in handling large-scale geospatial data and machine learning procedures offers promising avenues to potentially expedite and improve the accuracy of agricultural mapping in India. In this context, it becomes crucial to explore modern machine learning algorithms and cloud computing techniques, to generate precise SCI maps in an automated and functional manner. In light of these considerations, this study aimed to achieve a milestone by employing GEE and machine learning methods such as RF and CART for the inaugural classification of paddy crops and other land cover classes within a single district of Andhra Pradesh. This analysis involves the use of Sentinel satellite imagery captured in 2021. The information in these images can be used to create SCI charts and classify them into LC categories with an impressive spatial resolution of 10 m. The specific study presents a novel and comprehensive approach to mapping paddy cropland in the Guntur District, offering valuable insights into the integration of multiple data sources, machine learning, and cloud computing for agricultural and environmental monitoring. This study has practical applications for precision agriculture, land management, and policy development, ultimately contributing to sustainable and efficient land use in the region.

II. STUDY AREA

As shown in Figure 1, the research region includes one district in Andhra Pradesh, India, where paddy is grown within a small-scale rain-fed system in various agroecological situations. The field of study is surrounded by the Bay of Bengal on its southeast, Bapatla District on its south, Palnadu District on its west, NTR District on its northwest, and Krishna District on its northeastern boundary. Covering approximately 2,443 km^2 (943 mi^2), the area extends between 16.314209° N latitude and 80.435028° E longitude, with GPS coordinates of 16° 18' 51.1524" N latitude and 80° 26' 6.1008" E longitude. The Guntur district, where the study area is located, is primarily an agriculturally dominated region and occupies the fourth position in rice production. The region experiences tropical climatic conditions, with a yearly average temperature of 28.5°C (83.3°F) and an annual rainfall of approximately 905 mm (36 in). The influence of the southwest monsoon is evident throughout the area. During the monsoon season, June and July, the region experiences the highest monthly rainfall, with a maximum of 280 mm. In contrast, the 1 mm/month minimum rainfall is observed in December. The predominant agricultural practice is based on rain-fed paddy cultivation that is carried out during the winter months. This cultivation season extends from June to December, including paddy varieties with vegetation durations that typically range from 60 to 100 days.

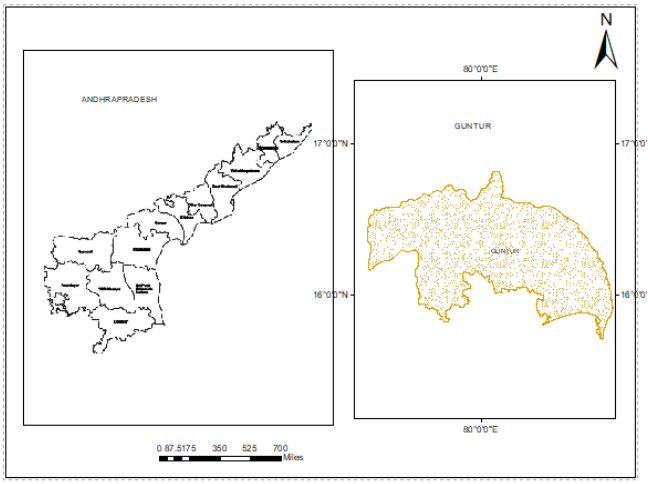

Fig. 1. Study area.

III. DATA AND PRELIMINARY PROCESSING

A. Sentinel-1 Satellite

The S1 Synthetic Aperture Radar (SAR) satellite constellation comprises two polar-orbiting satellites, with the initial satellite launched on April 3, 2014. The second satellite was launched on April 25, 2016, facilitated by a Europeanized Russian Soyuz rocket. The dual-polar metric outputs of the satellite's C-SAR instrument provide valuable assistance to researchers and users involved in agricultural analysis, LC/LU classification, and forestry. The S1 satellite's C-SAR instrument caters to both horizontal and vertical polarizations (HH, HV, VV, and VH), utilizing a single transmit chain that can be adapted to VH polarization. S1 Ground Range Detected (GRD) C-band imagery (at 5.405 GHz) was obtained through the Interferometry Wide swath (IW) mode. The IW mode enables coverage of a wide-swath width (250 km) that has a medium geometry density of 10 m. The GRD Level 1

processing encompasses tasks such as mitigating thermal noise and employing an Earth ellipsoid model for ground range projection. Each GRD product incorporates images in VH and/or VV polarization. The IW images exhibit a pixel spacing of 10 m, with azimuth incidence angles ranging from 30 to 45 degrees. In this study, paddy cultivation monitoring was carried out using microwave Sentinel-1A SAR data in three production areas within the Guntur district during the growing season of 2021. The IW mode S1A GRD images used in this study were sourced from the Google Earth Engine (GEE) platform, spanning from early June to December 2021 to facilitate temporal analysis. The period from June to October was chosen for cropland and vegetation type mapping. This timeframe encapsulates the entire paddy cultivation cycle, from the initial sowing to the eventual harvesting of the paddy crops.

B. Sentinel-2 Satellite

The categorization of the crops was carried out using the S2 Multi-Spectral Instrument (MSI) remote sensing satellite. Part of the Copernicus program, Sentinel-2 was developed by the European Space Agency (ESA), distinguished by its extensive coverage ranging from 10 to 60 m, spatial precision, multiple-spectrum capacity (encompassing 13 spectral bands), and frequent revisit cycles (ten days for one satellite and five days for a pair of satellites). The mission is well-equipped to monitor shifts in vegetation across growing seasons, oversee forest dynamics, identify land cover alterations, and provide swift responses to natural disasters. The main objective of the S2 mission is to methodically monitor terrestrial and coastal regions by providing quality visual imagery that covers vast areas and a higher review rate. This comprehensive spectral information, which spans visible, near-infrared, and shortwave infrared regions, significantly improves the ability to detect spatial and temporal fluctuations, as well as variations in vegetation status.

C. Rice Cultivation

In the Guntur district of Andhra Pradesh, paddy cultivation typically involves two primary seasons: Kharif (monsoon) and Rabi (winter). The Kharif season begins with the onset of monsoon rains in June and continues until October. The Rabi season occurs during the winter months, usually from November to February. These two seasons are the main paddy cultivation periods in the region. In general, the four monthly phases of rice growth are Tillage and Planting (T–P) (30 days), Vegetative growth (V) (30 days), reproductive (R) (30 days), and Maturity (M) (30 days).

IV. METHODOLOGY

Figure 2 shows the process steps used in this study for SCI mapping, which is based on the use of a machine-learning algorithm in conjunction with the Google Earth Engine platform. In the beginning, Regions of Interest (ROIs) were created for the location of rice fields in the Guntur district, Andhra Pradesh. These ROIs were established based on prior knowledge and verified utilizing very high-quality imagery from Google Earth. The size of the ROIs varied, with a geometric area measuring 11, 450, 082, 6.16 hectares. Data were collected for 15 days from S1 SAR, ensuring that it remained unaffected by cloud cover. However, the results did show a considerable noise-to-signal ratio. To address this issue, time series analysis was used to mitigate noise, particularly in regions where data scenes overlapped. For crop evaluation during the 2021 Kharif season, data from S1 and S2 were used. Ten VH values were extracted, considering them as distinct bands. By manipulating these bands, various color combinations indicative of different crop types, were derived. Subsequently, crop pixel boundaries within the ROIs were delineated using geometric polygons. The next step involved merging all the rice field crop polygons and establishing training points. Finally, machine learning algorithms were employed to classify the data into different crop categories.

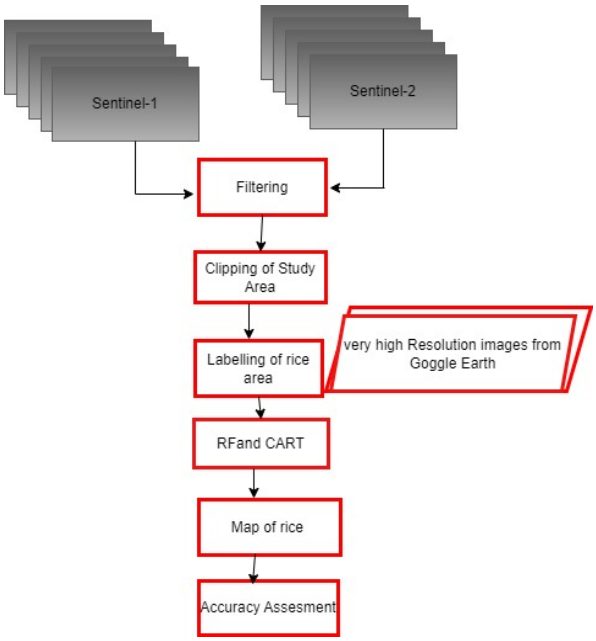

Fig. 2. Workflow diagram.

A. Accuracy Assessment

Accuracy assessment is a critical step in evaluating the reliability of a classification result. It involves measuring how closely the classification aligns with the actual true values. This assessment is typically carried out using confusion matrices that help calculate metrics such as Overall Accuracy (OA), Producer Accuracy (PA), and User Accuracy (UA) for crop maps. OA, for instance, is determined by comparing the proportion of reference pixels that were successfully classified to all correctly classified pixels. Analyzing the confusion matrix to understand the sources of discrepancies is an important and intriguing aspect of creating remote sensing maps. A built-in confusion matrix can be used in tools such as GEE to assess classifications in land cover types. This matrix allows a statistical comparison between the output classification and the ground truth associated with validation points.

B. Random Forest (RF)

RF is a powerful ensemble classifier that uses numerous individual decision trees to address the limitations of a single one. It makes classification decisions by aggregating the

majority "votes" from all trees. Instead of relying on a single tree, the RF incorporates multiple trees to achieve a more robust overall result. This ensemble approach helps mitigate the issues that can arise from a single tree's biases or errors. One of the notable strengths of RF is its ability to extract valuable information from each feature, contributing to its efficiency and accuracy. However, one drawback is that when using a large number of trees, it becomes challenging to visualize the individual trees due to their sheer quantity. This study used the GEE RF classifier to perform the classification. The particular approach highlights the versatility and effectiveness of RF in handling complex classification tasks.

C. Classification and Regression Tree (CART)

CART is a versatile algorithm capable of handling both classification and variable prediction tasks, much like RF. This algorithm falls within the realm of supervised machine learning, using training data to construct decision trees aiming to solve classification problems. In essence, the CART algorithm works by recursively dividing the data into subsets at each node of the tree based on the concept of normalized information gain. This normalized information gain is a key criterion for determining the attributes that define the splits in the tree. Ultimately, the final decision is made by selecting the attribute with the highest normalized information value, leading to effective classification or prediction outcomes. CART is particularly well suited for tasks involving remote sensing data, where it is often used. In the context of GEE, specific parameters such as the minimum number of leaves and the maximum number of nodes can be set to control the tree's complexity and optimize its performance.

D. F1- Score

The F1-Score is a valuable metric for evaluating classified maps. It is a statistical measure of accuracy derived from the confusion matrices, which contain reliability assessment statistics for each class. Equation (1) is used to calculate the F1-score, which represents the harmonic mean of precision and recall, fundamental metrics for assessing PA and UA. The F1-Score serves as a crucial measurement tool for assessing categorization models, offering advantages over independent UA/PA metrics. When it comes to accuracy assessment, both producers and consumers have their restrictions. Using a significant threshold can lead to more PA but significant data loss, while a low threshold may lead to elevated UA but less precise predictions. The F1-Score provides a more thorough analysis of a classifier while ensuring a balance between producer and user considerations.

$$F1 - Score = \frac{2 \times Precision \times Recall}{Precision + Recall} \quad (1)$$

V. RESULTS

The spatial distribution of paddy fields in Guntur district in 2021 was determined utilizing optical and SAR data chosen together. Both RF and CART algorithms were employed for this classification task. However, Figures 3 and 4 show that the paddy field distribution differs between the selected S1 and S2 data when employing these two algorithms for classification. Figures 3 and 4 represent pixel-based paddy crop field maps for 2021 using GEE, the RF and CART algorithms, and S1 and S2 imagery. The proposed approach effectively achieved the classification of paddy cropland through visual interpretation. Table I shows detailed pixel-based accuracy results for the chosen features extracted from S1 and S2 images. Based on S2 and S1 satellite data, paddy crop maps for 2021 were created with a 10 m resolution using the GEE platform. Based on the categorized result, it seems that most of the paddy pixels had been classified. The final ROI maps were visually sharp and noise-free due to post-processing to minimize noise. The suggested strategy allowed for relatively accurate identification and classification of paddy and other types using visual interpretation. Paddy crops can be detected effectively employing the suggested approach. This area has several rice fields where a substantial amount of paddy is produced each year. RF was compared to other classification algorithms such as CART. PA and UA were both 0.99% for the RF in the map created in 2021, while the OA and KC were each 0.97%. With the help of the Sentinel satellite data utilized, a respectable F-score was produced. Paddy has proven to have discriminatory talents (>0.90) during the year.

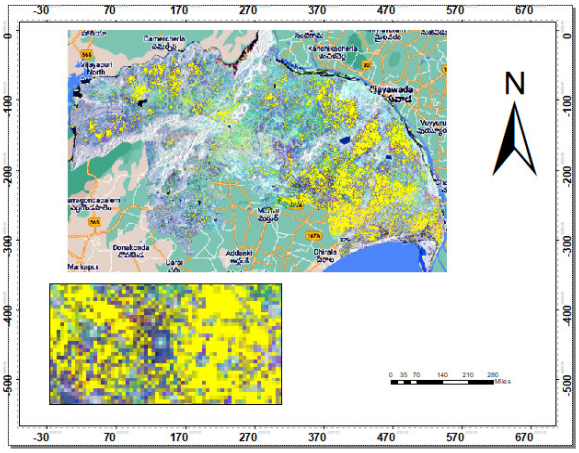

Fig. 3. Spatial mapping of paddy using RF.

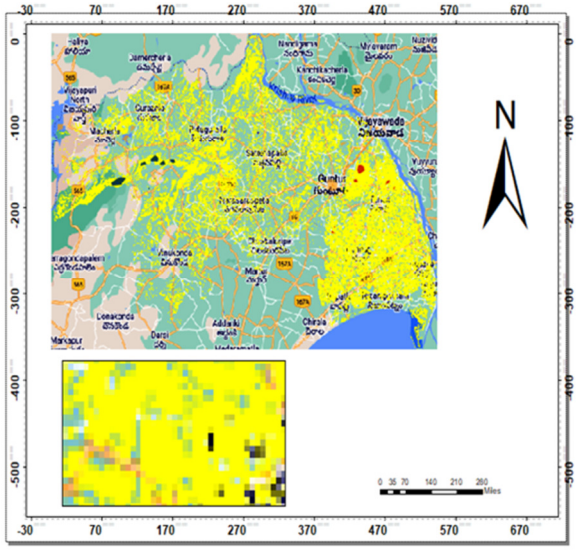

Fig. 4. Spatial mapping of paddy from S1 and S2 data using CART.

TABLE I. ACCURACY MAPS FOR 2021

LULC Name	2021RF		2021CART	
	User accuracy (%)	Producer accuracy (%)	User accuracy (%)	Producer accuracy (%)
Rice	0.99	0.99	0.80	0.81
OA	98		80	
F1-Score	98		80	

Considering different VH polarizations and the diverse development phases of paddy crops and other land cover categories, this study thoroughly investigated the seasonal and temporal variations in the S1 backscatter data. Figures 5 and 6 show the S1 SCI time series for VH polarization in ascending and descending orbits, respectively. These figures showcase the results obtained after processing and filtering the original S1 data to ensure accuracy. These findings indicate that the coefficient of backscattering in VH polarization for paddy fields falls within the range of 0 to 240 dB.

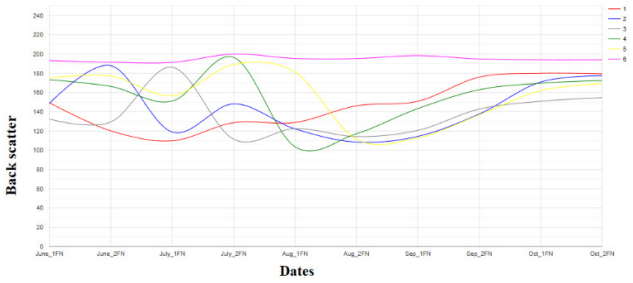

Fig. 5. Backscatter coefficient curves of RF.

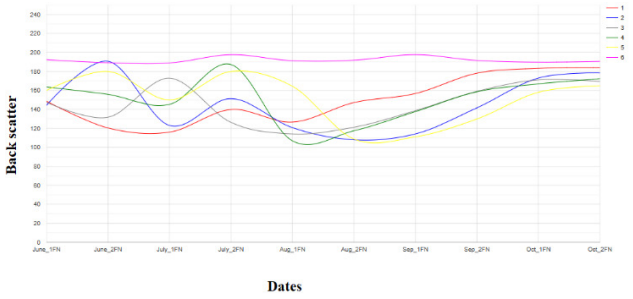

Fig. 6. Backscatter coefficient curves of CART.

VI. CONCLUSION

This study aimed to establish a comprehensive classification and mapping system to identify paddy crop areas and other categories in the Guntur region, India. It represents a pioneering effort in Guntur, exploring the capabilities of the GEE editor along with ML techniques using satellite imagery, specifically S1 and S2, within the paddy-producing areas in 2021. This approach used GEE to delineate paddy croplands and other land cover classes throughout the district, employing various classification algorithms such as RF and CART. The specific research effectively demonstrated the versatility and dependability of GEE for cropland mapping. To validate the findings, an average overall accuracy rate of 98% was achieved for the year 2021. These high levels of accuracy surpass the minimum requirements and are deemed reliable for pioneering research using GEE to build an SCI. This approach showcases a technological innovation that is not only efficient but also budget-friendly. The adoption of this method and the insights gained could have substantial implications for the development of Guntur Cropland Inventories (GCI) and the detection and identification of paddy crops. Future studies could seek to further enhance class accuracy by employing more advanced algorithms to map different crops outside of cropped regions.

REFERENCES

[1] L. Xu *et al.*, "Paddy Rice Mapping in Thailand Using Time-Series Sentinel-1 Data and Deep Learning Model," *Remote Sensing*, vol. 13, no. 19, 2021, https://doi.org/10.3390/rs13193994.

[2] *Dasar Agromakanan Negara 2011-2020*. Kementerian Pertanian dan Industri Asas Tani Malaysia, 2011, 2021.

[3] X. Xiao *et al.*, "Mapping paddy rice agriculture in South and Southeast Asia using multi-temporal MODIS images," *Remote Sensing of Environment*, vol. 100, no. 1, pp. 95–113, Jan. 2006, https://doi.org/10.1016/j.rse.2005.10.004.

[4] X. Xiao *et al.*, "Mapping paddy rice agriculture in southern China using multi-temporal MODIS images," *Remote Sensing of Environment*, vol. 95, no. 4, pp. 480–492, Apr. 2005, https://doi.org/10.1016/j.rse.2004.12.009.

[5] A. M. Shew and A. Ghosh, "Identifying Dry-Season Rice-Planting Patterns in Bangladesh Using the Landsat Archive," *Remote Sensing*, vol. 11, no. 10, 2019, https://doi.org/10.3390/rs11101235.

[6] J. Dong *et al.*, "Northward expansion of paddy rice in northeastern Asia during 2000–2014," *Geophysical Research Letters*, vol. 43, no. 8, pp. 3754–3761, 2016, https://doi.org/10.1002/2016GL068191.

[7] Z. Liu, Q. Hu, J. Tan, and J. Zou, "Regional scale mapping of fractional rice cropping change using a phenology-based temporal mixture analysis," *International Journal of Remote Sensing*, vol. 40, no. 7, pp. 2703–2716, Apr. 2019, https://doi.org/10.1080/01431161.2018.1530812.

[8] J. Dong *et al.*, "Tracking the dynamics of paddy rice planting area in 1986–2010 through time series Landsat images and phenology-based algorithms," *Remote Sensing of Environment*, vol. 160, pp. 99–113, Apr. 2015, https://doi.org/10.1016/j.rse.2015.01.004.

[9] K. Lasko, K. P. Vadrevu, V. T. Tran, and C. Justice, "Mapping Double and Single Crop Paddy Rice With Sentinel-1A at Varying Spatial Scales and Polarizations in Hanoi, Vietnam," *IEEE Journal of Selected Topics in Applied Earth Observations and Remote Sensing*, vol. 11, no. 2, pp. 498–512, Oct. 2018, https://doi.org/10.1109/JSTARS.2017.2784784.

[10] N. T. Son, C. F. Chen, C. R. Chen, and V. Q. Minh, "Assessment of Sentinel-1A data for rice crop classification using random forests and support vector machines," *Geocarto International*, vol. 33, no. 6, pp. 587–601, Jun. 2018, https://doi.org/10.1080/10106049.2017.1289555.

[11] H. Yang, B. Pan, W. Wu, and J. Tai, "Field-based rice classification in Wuhua county through integration of multi-temporal Sentinel-1A and Landsat-8 OLI data," *International Journal of Applied Earth Observation and Geoinformation*, vol. 69, pp. 226–236, Jul. 2018, https://doi.org/10.1016/j.jag.2018.02.019.

[12] H. Tian, M. Wu, L. Wang, and Z. Niu, "Mapping Early, Middle and Late Rice Extent Using Sentinel-1A and Landsat-8 Data in the Poyang Lake Plain, China," *Sensors*, vol. 18, no. 1, 2018, https://doi.org/10.3390/s18010185.

[13] L. R. Mansaray, D. Zhang, Z. Zhou, and J. Huang, "Evaluating the potential of temporal Sentinel-1A data for paddy rice discrimination at local scales," *Remote Sensing Letters*, vol. 8, no. 10, pp. 967–976, Oct. 2017, https://doi.org/10.1080/2150704X.2017.1331472.

[14] L. R. Mansaray, W. Huang, D. Zhang, J. Huang, and J. Li, "Mapping Rice Fields in Urban Shanghai, Southeast China, Using Sentinel-1A and Landsat 8 Datasets," *Remote Sensing*, vol. 9, no. 3, Mar. 2017, Art. no. 257, https://doi.org/10.3390/rs9030257.

[15] K. Clauss, M. Ottinger, and C. Kuenzer, "Mapping rice areas with Sentinel-1 time series and superpixel segmentation," *International*

Journal of Remote Sensing, vol. 39, no. 5, pp. 1399–1420, Mar. 2018, https://doi.org/10.1080/01431161.2017.1404162.

[16] J. D. Mohite *et al.*, "Operational Near Real Time Rice Area Mapping Using Multi-Temporal Sentinel-1 SAR Observations," *The International Archives of the Photogrammetry, Remote Sensing and Spatial Information Sciences*, vol. XLII–4, pp. 433–438, Sep. 2018, https://doi.org/10.5194/isprs-archives-XLII-4-433-2018.

[17] D. Mandal, V. Kumar, A. Bhattacharya, Y. S. Rao, P. Siqueira, and S. Bera, "Sen4Rice: A Processing Chain for Differentiating Early and Late Transplanted Rice Using Time-Series Sentinel-1 SAR Data With Google Earth Engine," *IEEE Geoscience and Remote Sensing Letters*, vol. 15, no. 12, pp. 1947–1951, Sep. 2018, https://doi.org/10.1109/LGRS.2018.2865816.

[18] D. B. Nguyen and W. Wagner, "European Rice Cropland Mapping with Sentinel-1 Data: The Mediterranean Region Case Study," *Water*, vol. 9, no. 6, 2017, https://doi.org/10.3390/w9060392.

[19] M. Saadat, M. Hasanlou, and S. Homayouni, "Rice Crop Mapping Using Sentinel-1 Time Series Images (Case Study: Mazandaran, Iran)," *The International Archives of the Photogrammetry, Remote Sensing and Spatial Information Sciences*, vol. XLII-4-W18, pp. 897–904, Oct. 2019, https://doi.org/10.5194/isprs-archives-XLII-4-W18-897-2019.

[20] M. Singha, J. Dong, G. Zhang, and X. Xiao, "High resolution paddy rice maps in cloud-prone Bangladesh and Northeast India using Sentinel-1 data," *Scientific Data*, vol. 6, no. 1, Apr. 2019, Art. no. 26, https://doi.org/10.1038/s41597-019-0036-3.

[21] S. Park, J. Im, S. Park, C. Yoo, H. Han, and J. Rhee, "Classification and Mapping of Paddy Rice by Combining Landsat and SAR Time Series Data," *Remote Sensing*, vol. 10, no. 3, 2018, https://doi.org/10.3390/rs10030447.

[22] Rudiyanto, B. Minasny, R. M. Shah, N. Che Soh, C. Arif, and B. Indra Setiawan, "Automated Near-Real-Time Mapping and Monitoring of Rice Extent, Cropping Patterns, and Growth Stages in Southeast Asia Using Sentinel-1 Time Series on a Google Earth Engine Platform," *Remote Sensing*, vol. 11, no. 14, 2019, https://doi.org/10.3390/rs11141666.

[23] V. N. Fikriyah, R. Darvishzadeh, A. Laborte, N. I. Khan, and A. Nelson, "Discriminating transplanted and direct seeded rice using Sentinel-1 intensity data," *International Journal of Applied Earth Observation and Geoinformation*, vol. 76, pp. 143–153, Apr. 2019, https://doi.org/10.1016/j.jag.2018.11.007.

[24] T. D. Setiyono *et al.*, "Rice yield estimation using synthetic aperture radar (SAR) and the ORYZA crop growth model: development and application of the system in South and South-east Asian countries," *International Journal of Remote Sensing*, vol. 40, no. 21, pp. 8093–8124, Nov. 2019, https://doi.org/10.1080/01431161.2018.1547457.

[25] N. Torbick, D. Chowdhury, W. Salas, and J. Qi, "Monitoring Rice Agriculture across Myanmar Using Time Series Sentinel-1 Assisted by Landsat-8 and PALSAR-2," *Remote Sensing*, vol. 9, no. 2, 2017, https://doi.org/10.3390/rs9020119.

[26] A. M. Ali *et al.*, "Integrated method for rice cultivation monitoring using Sentinel-2 data and Leaf Area Index," *The Egyptian Journal of Remote Sensing and Space Science*, vol. 24, no. 3, Part 1, pp. 431–441, Dec. 2021, https://doi.org/10.1016/j.ejrs.2020.06.007.

[27] N. You *et al.*, "The 10-m crop type maps in Northeast China during 2017–2019," *Scientific Data*, vol. 8, no. 1, Feb. 2021, Art. no. 41, https://doi.org/10.1038/s41597-021-00827-9.

[28] L. Liu *et al.*, "Mapping cropping intensity in China using time series Landsat and Sentinel-2 images and Google Earth Engine," *Remote Sensing of Environment*, vol. 239, Mar. 2020, Art. no. 111624, https://doi.org/10.1016/j.rse.2019.111624.

[29] R. Ni *et al.*, "An enhanced pixel-based phenological feature for accurate paddy rice mapping with Sentinel-2 imagery in Google Earth Engine," *ISPRS Journal of Photogrammetry and Remote Sensing*, vol. 178, pp. 282–296, Aug. 2021, https://doi.org/10.1016/j.isprsjprs.2021.06.018.

[30] S. Inoue, A. Ito, and C. Yonezawa, "Mapping Paddy Fields in Japan by Using a Sentinel-1 SAR Time Series Supplemented by Sentinel-2 Images on Google Earth Engine," *Remote Sensing*, vol. 12, no. 10, Jan. 2020, Art. no. 1622, https://doi.org/10.3390/rs12101622.

[31] M. Gatcha, F. Messelmi, and S. Saadi, "An Anisotropic Diffusion Adaptive Filter for Image Denoising and Restoration Applied on Satellite Remote Sensing Images: A Case Study," *Engineering, Technology & Applied Science Research*, vol. 12, no. 6, pp. 9715–9719, Dec. 2022, https://doi.org/10.48084/etasr.5363.

[32] Y. Slimani and R. Hedjam, "A Hybrid Metaheuristic and Deep Learning Approach for Change Detection in Remote Sensing Data," *Engineering, Technology & Applied Science Research*, vol. 12, no. 5, pp. 9351–9356, Oct. 2022, https://doi.org/10.48084/etasr.5246.

[33] M. K. Villareal and A. F. Tongco, "Multi-sensor Fusion Workflow for Accurate Classification and Mapping of Sugarcane Crops," *Engineering, Technology & Applied Science Research*, vol. 9, no. 3, pp. 4085–4091, Jun. 2019, https://doi.org/10.48084/etasr.2682.